

# Analytical interpretation of vertical interference pressure tests in stratified reservoirs

## Abstract

Vertical interference pressure tests in stratified reservoirs have commonly been interpreted using type-curve matching techniques which, although supported by rigorous mathematical formulations describing interlayer communication through low-permeability barriers, depend on graphical procedures that introduce subjectivity and reduce analytical flexibility. This work presents an analytical interpretation methodology for vertical interference pressure tests based on Tiab's Direct Synthesis (*TDS*) technique as an alternative to conventional curve-matching approaches. A classical vertical interference model was implemented computationally to generate dimensionless pressure and pressure-derivative responses, allowing systematic evaluation of the effects of the governing dimensionless parameters  $\lambda$ ,  $K$  and  $\omega$  on transient flow behavior. Characteristic points were identified on log-log pressure and pressure-derivative plots, and normalization relationships were developed to collapse responses corresponding to different parameter values into unified trends from which direct analytical expressions were obtained. The proposed methodology enables estimation of vertical communication and individual layer permeabilities directly from pressure transient data without reliance on type-curve matching. Validation using reference and synthetic cases produced consistent parameter estimates and confirmed the applicability of the *TDS* technique to vertically communicating stratified reservoir systems. The methodology provides an objective and reproducible framework for interpreting vertical interference pressure tests in multilayer reservoirs with vertical communication.

Volume 8 Issue 1 - 2026

Ingris Astrid Mendoza, Freddy Humberto Escobar, Juan Pablo Salazar

Department of Petroleum Engineering, Universidad Surcolombiana, Colombia

**Correspondence:** Dr. Freddy H Escobar, Petroleum Engineering Department, Universidad Surcolombiana, Colombia, Tel+57 3154195526

**Received:** February 09, 2026 | **Published:** April 3, 2026

## Introduction

The determination of vertical communication between stratigraphic layers is a fundamental aspect of reservoir engineering, since the existence of crossflow through low-permeability layers directly controls the efficiency of several exploitation and enhanced oil recovery (EOR) processes. Quantifying this hydraulic continuity is essential for evaluating the interaction between flow units, estimating vertical permeability  $k_z$ , and properly characterizing interlayer transmissibility. For this purpose, the petroleum industry has developed and applied specialized pressure tests capable of dynamically revealing the degree of vertical communication present in a reservoir.

The concept of using well configurations to evaluate vertical communication was formally established by Earlougher,<sup>1</sup> who defined so-called vertical interference tests as single-well tests in which two sets of intervals are hydraulically isolated, one acting as the active zone and the other as the observation zone, with the objective of estimating vertical permeability -an attribute that, until then, had been difficult to determine dynamically-. In parallel, the mathematical analysis of pressure interference advanced significantly with the work of Tiab & Kumar,<sup>2</sup> who introduced the use of dimensionless pressure functions to interpret the pressure response between a source well and an observation well, enabling the calculation of system transmissibility and storage.

These contributions are framed within the broader development of pressure transient analysis (PTA), one of the most important tools in reservoir engineering for dynamic reservoir characterization. PTA allows the estimation of fundamental properties such as permeability, effective porosity, and initial reservoir pressure, as well as the diagnosis of well condition through the identification of formation damage (skin), and the evaluation of hydraulic connectivity with boundaries or aquifers. The theoretical foundation of these techniques

lies in the solution of the diffusivity equation for flow in porous media, derived from the combination of Darcy's law and the principle of mass conservation. Under conditions of radial flow in a homogeneous and infinite medium, the analytical solution is expressed through the exponential integral function, known as the line-source solution. This framework is analogous to the solution proposed by Theis,<sup>3</sup> in hydrogeology and was formally adapted to petroleum engineering by Muskat,<sup>4</sup> and, later by Van Everdingen & Hurst.<sup>5</sup>

Methodological advances in PTA were consolidated with the introduction of the semilogarithmic plot by Horner,<sup>6</sup> a technique designed for the interpretation of pressure buildup tests following extended production periods. This development complemented earlier work by Copper, Jr & Jacob,<sup>7</sup> on straight-line analysis and the early use of type curves. Subsequently, the discipline incorporated more robust mathematical tools, notably Green's functions and Laplace transforms, as demonstrated by Gringarten & Ramey.<sup>8</sup> These analytical frameworks enabled the treatment of complex flow geometries and reservoir heterogeneities and were later refined through advanced data-processing algorithms, most notably the pressure-derivative function introduced by Tiab & Kumar.<sup>2</sup>

Within this general framework, interference tests represent a specific category of transient tests in which a pressure disturbance induced at an active well generates a pressure response at one or more observation wells, allowing the evaluation of hydraulic communication within the system. In stratified reservoirs, these tests are particularly important due to the presence of layers with contrasting permeabilities, where vertical crossflow through semipermeable barriers is frequently observed. This phenomenon occurs when pressure differentials exist between layers, breaking hydraulic isolation and allowing vertical fluid movement. Quantifying this process is essential for accurately representing the reservoir in simulation models and for reliably estimating vertical permeability.

Over the decades, several analytical approaches have been developed to interpret such tests. Burns,<sup>9</sup> introduced a single-well pulse test to determine vertical permeability, followed by Prats,<sup>10</sup> who proposed a similar method to estimate net vertical permeability using in situ measurements. Later, Hirasaki,<sup>11</sup> reviewed and generalized these approaches within the context of early-time transient tests. These classical studies established the fundamental physical principle that a pressure change in one layer generates gradients that induce vertical flow through low-permeability barriers.

For the specific case of two permeable layers separated by a thin, very low-permeability barrier, more rigorous analytical models were developed. Bremer et al.<sup>12</sup> presented a linearized diffusion model for vertical interference tests, commonly referred to as the narrow-zone model, which relied on type-curve interpretation. Building upon this work, Ehlig-Economides & Ayoub,<sup>13</sup> extended the model by incorporating distinct properties for each layer, as well as wellbore storage and skin effects, providing a rigorous mathematical solution that constitutes the base model of the present study. Similarly, Hatzignatiou & Ogbe,<sup>14</sup> presented analytical solutions in the Laplace domain for stratified formations with different layer properties.

In recent decades, pressure transient analysis has continued to evolve with the development of advanced interpretation methodologies and improved numerical tools capable of addressing increasingly complex reservoir architectures. Modern PTA approaches integrate derivative-based diagnostics, deconvolution techniques, and multiwell testing strategies to improve the identification of flow regimes and reservoir heterogeneities. Comprehensive treatments of these developments are presented in the works of Bourdet<sup>15</sup> Kuchuk<sup>16</sup> and Tiab & Donaldson,<sup>17</sup> which describe analytical and practical frameworks for interpreting pressure responses in heterogeneous and multilayer systems. These contributions have demonstrated that transient pressure data remain one of the most powerful dynamic sources of information for reservoir characterization, particularly in stratified formations where vertical communication and crossflow between layers strongly influence the observed pressure behavior.

The novelty of this work lies in extending the analytical capabilities of the Tiab's Direct Synthesis (*TDS*) technique to the interpretation of vertical interference tests in stratified reservoirs with crossflow. Traditionally, the interpretation of such systems has relied on type-curve matching procedures derived from the models of Bremer et al.<sup>12</sup> and Ehlig-Economides and Ayoub.<sup>13</sup> Although physically rigorous, these methods require graphical matching and iterative adjustments that introduce subjectivity into the interpretation process. In contrast, the *TDS* technique is based on the direct use of characteristic features of the pressure-derivative plot, allowing reservoir parameters to be obtained through analytical expressions derived from identifiable points such as derivative plateaus, minima, maxima, and intersection points. The methodology developed in this work demonstrates that the vertical interference model can be interpreted exclusively from the derivative behavior, eliminating the need for type-curve matching and reducing interpretation ambiguity. Additionally, several reservoir parameters can be independently estimated from different characteristic points on the derivative curve, which provides internal consistency checks and improves the robustness of the interpretation. Therefore, the main contribution of this study is the formulation of a direct analytical interpretation methodology that integrates the classical vertical interference model with the *TDS* framework, enabling a more objective, reproducible, and practical characterization of stratified reservoirs with vertical communication.

Despite their strong physical foundation, these models have traditionally been interpreted using type curves, which introduces

subjectivity and limits the precise identification of flow regimes, particularly in stratified systems with crossflow. This limitation motivated a conceptual shift in pressure-test interpretation with the introduction of the *TDS* (Tiab's Direct Synthesis) technique by Tiab.<sup>18,19</sup> This methodology is based on the joint analysis of pressure and pressure-derivative responses, allowing the identification of unique characteristic points that act as dynamic fingerprints of reservoir behavior and enabling the direct analytical estimation of key parameters without reliance on graphical type-curve matching. More recently, Escobar et al.<sup>20</sup> validated the application of the *TDS* technique to multiwell interference tests in reservoirs exhibiting crossflow.

In this context, the present research integrates the classical vertical interference model of Ehlig-Economides & Ayoub,<sup>13</sup> with the modern Tiab's Direct Synthesis (*TDS*) interpretation technique. The original mathematical formulation of the model was not modified; instead, it was computationally implemented to generate synthetic dimensionless pressure and pressure-derivative responses that describe the transient behavior of stratified reservoirs with vertical communication. Based on these responses, a systematic normalization and analysis procedure was carried out to identify characteristic points on the pressure-derivative curves and to derive analytical relationships among the governing parameters of the system. The objective of this study is therefore to develop a direct analytical interpretation methodology for vertical interference tests using the *TDS* technique, enabling the estimation of vertical communication and individual layer permeabilities directly from pressure-derivative behavior, while eliminating the need for subjective type-curve matching procedures.

## Mathematical model

In the vertical interference model, the dimensionless parameters  $\kappa$ ,  $\lambda$  and  $\omega$  describe the relative hydraulic properties of the layered system and control the transient pressure behavior observed during the test. The parameter  $\kappa$  represents the ratio of the horizontal flow capacities of the two layers and therefore quantifies the contrast in permeability–thickness between them; large values of  $\kappa$  indicate that one layer dominates the horizontal flow, while values near unity imply similar transmissibility in both layers. The parameter  $\omega$  represents the relative storage capacity of the layers, combining porosity, compressibility, and thickness, and determines how fluid expansion and storage effects are distributed between the zones during the transient process. Finally,  $\lambda$  is the vertical communication parameter, which characterizes the transmissibility of the low-permeability barrier separating the layers and therefore controls the magnitude and timing of crossflow between them. When  $\lambda$  is very small, the barrier strongly restricts vertical flow and the layers behave almost independently, whereas larger values of  $\lambda$  indicate stronger hydraulic communication and a faster pressure equilibration between layers. Together, these parameters describe the balance between horizontal flow within each layer and vertical crossflow across the separating zone, which ultimately governs the pressure-transient response of the stratified system.

In the model proposed by Ehlig-Economides & Ayoub,<sup>13</sup> for vertical interference testing between two permeable layers separated by a very low-permeability zone, a slightly compressible fluid with constant viscosity is assumed. Horizontal flow in each layer is governed by Darcy's law, neglecting the quadratic pressure-gradient term. Under these conditions, the modified diffusivity equations are formulated to account for vertical flow (crossflow) between the layers. The physical domain of the model, including the two permeable layers and the intervening low-permeability barrier, is schematically illustrated in Figure 1. The model introduces three key dimensionless parameters

$-\kappa, \lambda$ , and  $\omega$  – which encapsulate the relative properties of each layer and the characteristics of vertical flow. Specifically,  $\kappa$  represents the relative flow capacity of each layer,  $\omega$  quantifies the relative storage capacity, and  $\lambda$  characterizes the ease of vertical flow across the low-permeability barrier. The dimensionless definitions used to describe these properties are presented below:

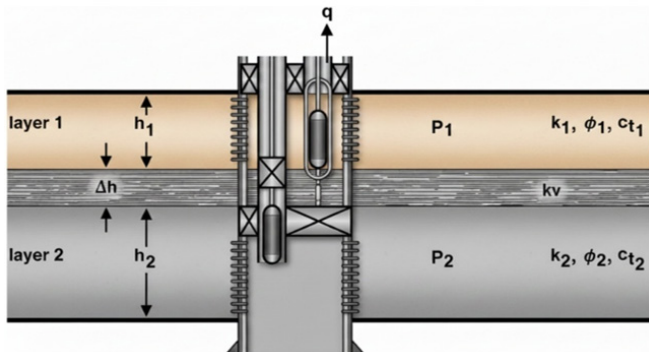


**Figure 1** Conceptual model of a single-well vertical interference test across a low-permeability zone, Ehlig-Economides & Ayoub.<sup>13</sup>

$$\kappa = \frac{k_1 h_1}{k_1 h_1 + k_2 h_2} \quad (1)$$

$$\omega = \frac{(\phi c_i h)_1}{(\phi c_i h)_1 + (\phi c_i h)_2} \quad (2)$$

$$\lambda = \frac{r_w^2 k_v}{(kh)_1 + (kh)_2 \Delta h} \quad (3)$$

The dimensionless quantities are defined as:

$$P_D = \frac{(k_1 h_1 + k_2 h_2) \Delta P}{141.2 q \mu B} \quad (4)$$

$$t_D * P_D' = \frac{(k_1 h_1 + k_2 h_2) (t * \Delta P)'}{141.2 q \mu B} \quad (5)$$

$$t_{vD} = \frac{0.0002637 (k_1 h_1 + k_2 h_2) t}{(\phi c_i h)_1 + (\phi c_i h)_2 \mu r_w^2} \quad (6)$$

$$r_D = \frac{r}{r_w} \quad (7)$$

$$C_{vD} = \frac{0.89359 C}{[(\phi c_i h)_1 + (\phi c_i h)_2] r_w^2} \quad (8)$$

$$k_v = \frac{\lambda \Delta h \bar{k} h}{r_w^2} \quad (9)$$

The solution for the pressure distribution as a function of radial distance from the well is given by:

$$\bar{P}_D - \bar{P}_{2D} = \left( \frac{1}{\ell - C_{vD} \ell \bar{P}_{vD}} \right) \left\{ \frac{1}{\kappa (a_2 - a_1)} \left[ (a_2 - 1) \frac{K_0(\sigma_2 r_D)}{\sigma_2 K_1(\sigma_2)} - (a_1 - 1) \frac{K_0(\sigma_1 r_D)}{\sigma_1 K_1(\sigma_1)} \right] \right\} \quad (10)$$

Where,

$$a_{1,2} = \frac{(1 - \kappa) \left[ \frac{(1 - \omega) \ell + \lambda}{1 - \kappa} - \sigma_{1,2}^2 \right]}{\lambda} \quad (11.a)$$

$$\sigma_{1,2}^2 = \frac{1}{2} \left[ \frac{(1 - \omega) \ell + \lambda}{1 - \kappa} + \frac{\omega \ell + \lambda}{\kappa} \right] \pm \frac{1}{2} \left\{ \left[ \frac{(1 - \omega) \ell + \lambda}{1 - \kappa} - \frac{\omega \ell + \lambda}{\kappa} \right]^2 + \frac{4 \lambda^2}{\kappa (1 - \kappa)} \right\}^{1/2} \quad (11.b)$$

$$K_1^0(z) = K_0(z) / [z K_1(z)] \quad (12)$$

## Analytical methodology for pressure test interpretation using the TDS technique

The analytical formulation of the interpretation methodology based on Tiab's Direct Synthesis technique (TDS) presented here was originally developed as part of the Master's thesis research conducted by Mendoza,<sup>21</sup>

The dimensionless quantities considered for the development of the present work are detailed below:

$$t_D = \frac{0.0002637 k t}{\phi \mu c_i r_w^2} \quad (13)$$

$$C_D = \frac{0.89359 C}{\phi c_i h r_w^2} \quad (14)$$

Tiab<sup>19</sup> presented the following expressions:

$$k = \frac{70.6 q \mu B}{h_i (t * \Delta P)'_r} \quad (15)$$

$$C = \frac{k h t_i}{1695 \mu} \quad (16)$$

$$s = 0.5 \left( \frac{(\Delta P)'_r}{(t * \Delta P)'_r} - \ln \left[ \frac{k t_r}{\phi \mu c_i r_w^2} \right] + 7.43 \right) \quad (17)$$

During radial flow, the dimensionless pressure derivative takes a value of 0.5. Under this condition, Equation (5) allowed finding:

$$k_2 = \left( \frac{70.6 q \mu B}{(t * \Delta P)'_r} - k_1 h_1 \right) \frac{1}{h_2} \quad (18)$$

In Figure 2, the behavior of  $(t_D * P_D)'$  is observed for different values of  $\lambda$ . At very low values of  $\lambda$  (low-permeability layer or a very thick barrier), the layers are practically isolated, and fluid transfer between zones during the transient period is negligible. Each layer responds almost independently, exhibiting behavior characteristic of separate reservoirs. Conversely, at higher values of  $\lambda$  (a barrier with good transmissibility), the layers behave nearly as a single unit, as pressure equilibrates rapidly and the system responds as a combined reservoir.

With the purpose of obtaining a unified representation of the pressure and pressure-derivative responses and to facilitate the identification of characteristic points and analytical relationships, a normalization procedure was applied to the governing variables. Specifically, the dimensionless time was scaled by the vertical transmissibility parameter  $\lambda$ , such that the responses corresponding to different values of  $\lambda$  collapse onto a common trend. This

normalization reduces the apparent dispersion among the curves and highlights the intrinsic dynamic behavior of the system, allowing the extraction of characteristic times and invariant features suitable for analytical interpretation within the framework of the TDS Technique.

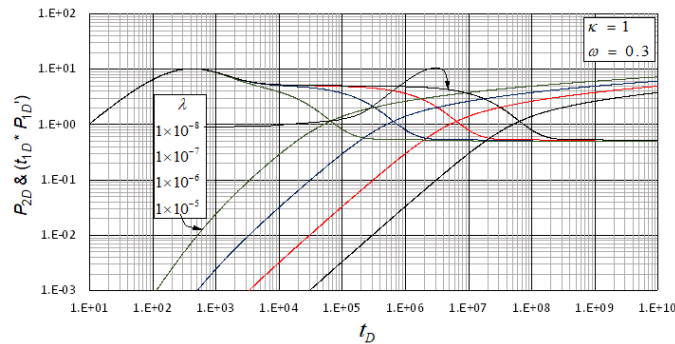


**Figure 2** Dimensionless pressure in zone 2 and dimensionless pressure derivative in zone 1 versus dimensionless time log-log plot for different values of  $\lambda$ .

In Figure 3, a unique intersection point between  $t_D * P_D'$  for Zone 1 and  $P_D$  for Zone 2 is identified. This point is denoted as  $t_{(\Delta P_2 - (t^* \Delta P^*))_i}$ . The intersection point was normalized by applying the scaling  $t_{1D} \lambda$  and  $t_{1D} \lambda$ , yielding:

$$t_D \lambda = 0.628 \quad (19)$$

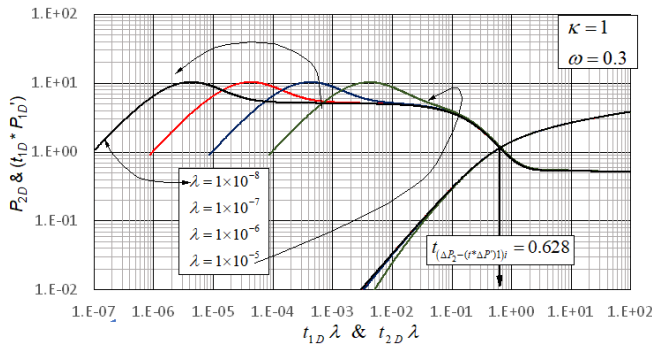


**Figure 3** Unified behavior of the dimensionless pressure derivative curves for Zone 1 and dimensionless pressure for Zone 2 versus dimensionless times multiplied by  $\lambda$  log-log plot for different values of  $\lambda$ .

After substituting Equation (13) into Equation (19) and solving for  $\lambda$ , the following expression was obtained, which allows calculation of the vertical communication factor  $\lambda$ :

$$\lambda = 2381.494 \left( \frac{\phi_i \mu c_f r_w}{k_1 t_{(\Delta P_2 - (t^* \Delta P^*))_i}} \right) \quad (20)$$

The normalization procedure applied in this study is based on the principle of dynamic similarity in dimensionless transient solutions. For a given governing parameter  $X$ , families of pressure and pressure-derivative curves obtained for different values of  $X$  exhibit similar shapes but are shifted along the time and/or pressure axes. This behavior indicates that the solutions differ primarily by a scaling factor associated with the influence of the parameter on the governing diffusivity equation. Consequently, a rescaling of the variables is performed by multiplying the dimensionless time and pressure quantities by powers of the parameter  $X$ , such that  $t_D X^x$  and  $P_D X^y$ . The exponents  $x$  and  $y$  are determined iteratively until the responses

corresponding to different values of the parameter converge into a single unified trend, revealing invariant characteristic points that can be used for analytical interpretation. This procedure does not alter the physical nature of the solution but rather highlights the intrinsic similarity of the transient responses controlled by the parameter under study. A similar normalization strategy has been successfully applied in pressure-transient interpretation problems involving anisotropic systems, where the rescaling of dimensionless variables allows different solutions to be represented by a single master behavior Escobar et al.<sup>22</sup>

The porosity–compressibility–thickness product  $\omega$  reflects the relative fluid storage capacity of one layer with respect to the other. High values of  $\omega$  indicate a larger storage capacity in the secondary layer, which delays pressure redistribution between layers and prolongs the early-time radial flow regime. In contrast, low values of  $\omega$  reduce the storage capacity, accelerate the establishment of vertical hydraulic equilibrium, and promote the early onset of the infinite-acting radial flow regime of the coupled system. This effect is illustrated in Figure 4.

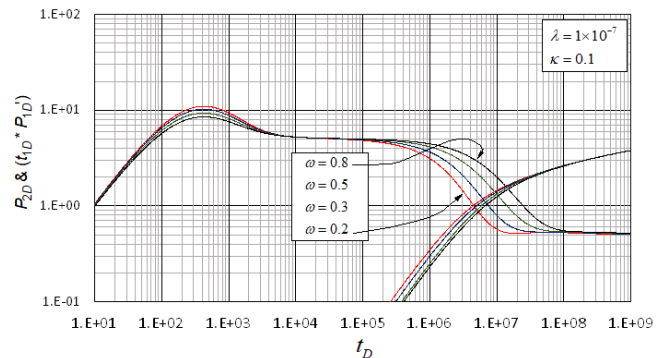


**Figure 4** Dimensionless pressure in zone 2 and dimensionless pressure derivative in zone 1 versus dimensionless time log-log plot for different values of  $\omega$ .

After applying the normalization defined as  $t_{1D} / \omega^{1.18}$  and  $t_{2D} / \omega^{0.25}$ , Figure 5 shows that a unique intersection point once again emerges between  $t_D * P_D'$  for Zone 1 and  $P_D$  for Zone 2. This intersection point is denoted as  $t_{(\Delta P_2 - (t^* \Delta P^*))_i}$ . The collapse of the curves onto a common trend confirms the adequacy of the proposed normalization and enables the definition of a characteristic time independent of  $\omega$ , from which the analytical expression presented below is derived.

$$\frac{t_D}{\omega^{1.18}} = 1.8 \times 10^7 \quad (21)$$

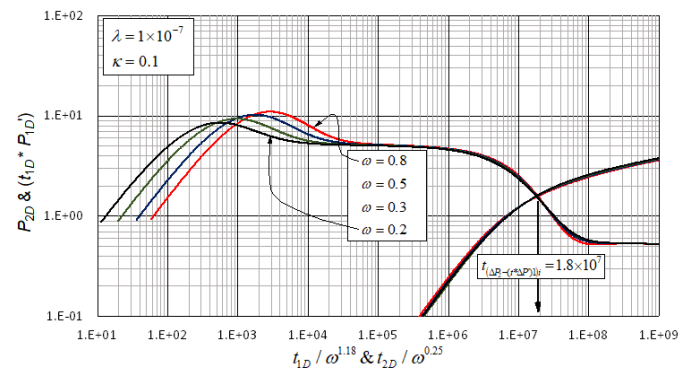


**Figure 5** Unified behavior of the dimensionless pressure derivative for Zone 1 and dimensionless pressure for Zone 2 versus dimensionless times multiplied by  $\omega^{-1.18}$  and  $\omega^{-0.25}$  log-log plot for different values of  $\omega$ .

Equation (13) was substituted into Equation (19), and the resulting expression was rearranged to solve for  $w$ , yielding a formulation suitable for calculating the porosity–compressibility–thickness product, as shown below:

$$\omega = 6.584 \times 10^{-10} \left( \frac{kt(\Delta P_2 - (t^* \Delta P')_1) i}{\phi \mu c_t r_w} \right)^{0.85} \quad (22)$$

In Figure 6, it is observed that the parameter  $\kappa$  controls the contrast in flow capacity between the zones. As  $\kappa$  increases, the difference between flow capacities becomes larger, which intensifies internal fluid redistribution once vertical communication is established. This process manifests itself as a transient depression in the pressure derivative, whose shape is analogous to the response commonly observed in naturally fractured systems. In contrast, for lower values of  $\kappa$ , where the flow capacities of the zones are comparable, the transition is more gradual and the response departs from behavior characteristic of naturally fractured reservoirs.

With reference to the response shown in Figure 6, an empirical rescaling of  $t_D$  and  $t_D^* P_D'$  was applied to collapse the transient responses associated with the minimum of the pressure derivative for different values of the parameter  $\kappa$ . The adjustment was performed specifically in the vicinity of the minimum of  $t_D^* P_D'$ , since this point is representative of the internal flow redistribution regime and is highly sensitive to the contrast in flow capacity between the zones, as quantified by  $\kappa$ .

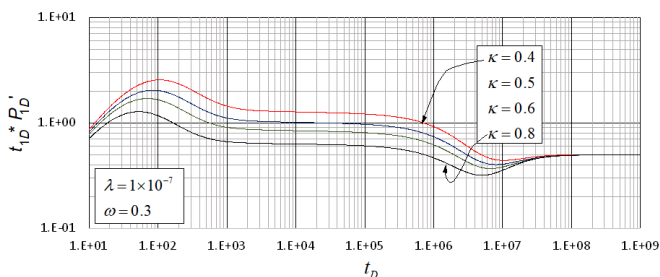


**Figure 6** Dimensionless pressure derivative in zone 1 versus dimensionless time log-log plot for different values of  $\kappa$

The minimum observed in the pressure-derivative curve is directly associated with the transient redistribution of flow between the two layers once vertical communication begins to influence the system response. At early times, the pressure behavior is dominated by radial flow within the producing layer, and the derivative follows the characteristic radial-flow plateau. As the pressure disturbance propagates through the low-permeability barrier, vertical crossflow between the layers becomes progressively significant, causing part of the fluid to be redistributed toward the second layer. This redistribution temporarily reduces the rate of pressure decline in the producing layer, producing a depression in the pressure-derivative curve. The magnitude and timing of this minimum are strongly controlled by the parameter  $\kappa$ , which represents the contrast in flow capacity between the layers. When  $\kappa$  is large, indicating a stronger hydraulic contrast, the redistribution of flow between zones is more pronounced and the derivative minimum becomes deeper and more clearly defined. Conversely, when  $\kappa$  approaches unity, the flow capacities of both layers are similar and the transition between flow regimes becomes smoother, reducing the prominence of the minimum. Therefore, the derivative minimum acts as a diagnostic feature that reflects the hydraulic interaction between layers and provides a practical indicator for estimating the permeability contrast within the stratified system.

The rescaling was carried out using the transformations  $t_{1D}\kappa$  and  $(t_{1D}^* P_{1D}')\kappa^{0.45}$ , as illustrated in (Figure 7). These transformations allowed the curves corresponding to different values of  $\kappa$  to be properly superimposed around the derivative minimum. This procedure demonstrates that the amplitude of the minimum is primarily controlled by the hydraulic contrast between the zones and can be normalized through appropriate powers of  $\kappa$ .

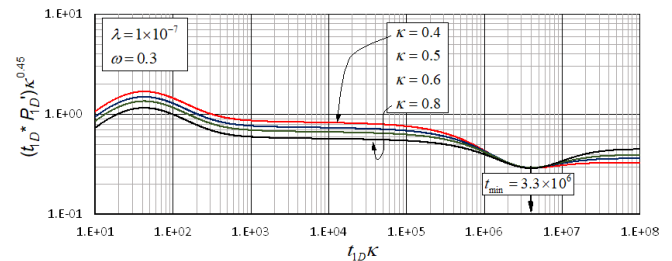


**Figure 7** Unified behavior of the dimensionless pressure derivative for zone 1 multiplied by  $\kappa^{0.45}$  versus dimensionless time multiplied by  $\kappa$  log-log plot for different values of  $\kappa$ .

It should be emphasized that this adjustment does not alter the physical nature of the flow regime. Rather, it constitutes a dimensionless normalization intended to highlight the dynamic similarity of the vertical interference process, analogous to the behavior observed in naturally fractured systems. The value of  $t_D$  at the identified minimum was  $3.3 \times 10^6$ ; equating this value to the proposed rescaling yields the following expression:

$$t_D \kappa = 3.3 \times 10^6 \quad (23)$$

Subsequently, Equation (13) was substituted into Equation (23), and the time variable was defined as  $(t_1)_{\min}$ , from which the following expression, valid for the calculation of  $t_1$ , was obtained:

$$\kappa = 1.25 \times 10^{10} \left( \frac{\phi \mu c_t r_w^2}{k(t_1)_{\min}} \right) \quad (24)$$

Finally, by using Equations (15) and (18), the following expressions can be obtained to calculate  $k_1$  from  $\kappa$ , and  $k_2$  once  $k_1$  is known:

$$k_1 = \frac{70.6q\mu B}{(t^* \Delta P')h_1} \quad (25)$$

The identification of characteristic points on log–log plots of pressure and pressure derivative may be affected by uncertainties associated with data quality and derivative calculation. In practice, field pressure data frequently contain measurement noise, rate fluctuations, or operational disturbances that can distort the shape of the derivative curve and obscure diagnostic features such as plateaus, minima, or intersection points. In addition, numerical differentiation of pressure data inherently amplifies high-frequency noise, particularly when inappropriate derivative algorithms or insufficient data smoothing procedures are used. These effects may introduce uncertainty in the precise location of characteristic points used in analytical interpretation methods such as *TDS*. To mitigate these issues, derivative calculations should be performed using robust algorithms designed for well-test analysis, together with appropriate filtering or smoothing techniques that preserve the underlying transient behavior while reducing noise amplification. When such procedures are applied, the main diagnostic features of the pressure-derivative curve remain sufficiently stable to allow reliable identification of characteristic points and consistent estimation of reservoir parameters.

## Examples

### Field example

Ehlig-Economides & Ayoub,<sup>13</sup> presented an example which relevant data are given in Table 1.

**Table 1** Input data for field example

$q = 2000$ bpd	$r_w = 0.25$ ft	$B_o = 1.278$ rb/stb	$\phi_1 = 0.0201$
$\phi_2 = 0.214$	$\mu = 1.358$	$c_i = 1.023 \times 10^{-5}$ psi-l	$h_1 = 18$ ft
$h_2 = 7$ ft	$\Delta h = 4.5$ ft		

Figure 8 presents the log-log plot of pressure and pressure derivative versus time for both  $P_1$  and  $P_2$ . The following data are read from such plot:

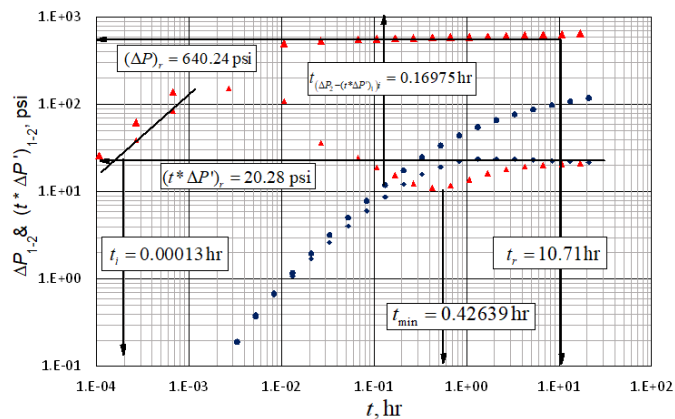


**Figure 8** Pressure and pressure derivative versus time log-log plot for field example, Ehlig-Economides & Ayoub.<sup>13</sup>

$$t_r = 10.71 \text{ hr} \quad (t^* \Delta P^*)_r = 20.28 \text{ psi} \quad \Delta P_r = 640.24 \text{ psi}$$

$$t_i = 0.00013 \text{ hr} \quad t_{min} = 0.42639 \text{ hr} \quad t(\Delta P_2 - (t^* \Delta P^*)_1) = 0.16975 \text{ hr}$$

Find  $k$  with Equation (15):

$$k = \frac{70.6(2000)(1.358)(1.278)}{(20.28)(18)} = 671.31 \text{ md}$$

Find with Equation (24) and  $k_1$  by means of Equation (25):

$$\kappa = 1.25 \times 10^{10} \left( \frac{(0.0201)(1.358)(1.023 \times 10^{-5})(0.25^2)}{(671.31)(0.42639)} \right) = 0.76213$$

$$k_1 = 0.76213 \left( \frac{(70.6)(2000)(1.358)(1.278)}{(20.28)(18)} \right) = 511.6 \text{ md}$$

Using the obtained values of  $k_1, k_2$  was calculated with Equation (18), yielding:

$$k_2 = \left( \frac{(70.6)(2000)(1.358)(1.278)}{(20.28)} - (511.6)(18) \right) \frac{1}{7} = 411 \text{ md}$$

Calculate  $\lambda$  and  $\omega$  using Equations (20) and (22), respectively:

$$\lambda = 2381.494 \left( \frac{(0.0201)(1.358)(1.023 \times 10^{-5})(0.25^2)}{(511.6)(0.16975)} \right) = 4.79 \times 10^{-7}$$

$$\omega = 6.584 \times 10^{-10} \left( \frac{(511.6)(0.16975)}{(0.0201)(1.358)(1.023 \times 10^{-5})(0.25^2)} \right)^{0.85} = 0.115$$

Subsequently, using the obtained value of  $\lambda, k_v$  was calculated with Equation (9):

$$k_v = \frac{4.79 \times 10^{-7} (4.5) [(511.6)(18) + (411)(7)]}{0.25^2} = 0.416 \text{ md}$$

Finally, wellbore storage and skin factor were estimated with Equations (16) and (17), respectively:

$$C = \frac{511.6(18)(0.00013)}{1695(1.358)} = 0.000520 \text{ bbl/psi}$$

$$s = 0.5 \left( \frac{(630.68)}{(20.28)} - \ln \left[ \frac{(511.6)(6.75)}{(0.0201)(1.358)(1.023 \times 10^{-5})(0.25^2)} \right] + 7.43 \right) = 6.26$$

Results are reported in Table 2 and are compared against Ehlig-Economides & Ayoub.<sup>13</sup>

**Table 2** Comparison of results for field example

Parameter	Results from:	
	Ehlig-Economides & Ayoub <sup>13</sup>	This work
$\kappa$	0.8026	0.7621
$\omega$	0.1945	0.14657
$\lambda$	$5.66 \times 10^{-7}$	$3.56 \times 10^{-7}$
$s$	3.67	5.76
$C$ , bbl/psi	0.000422	0.00068
$k_1$ , md	511	511
$k_2$ , md	323	411
$k_v$ , md	0.467	0.317

### Synthetic example

Figure 9 reports a pressure drop and pressure derivative versus time data for a well generated with the input data provided in Table 3:

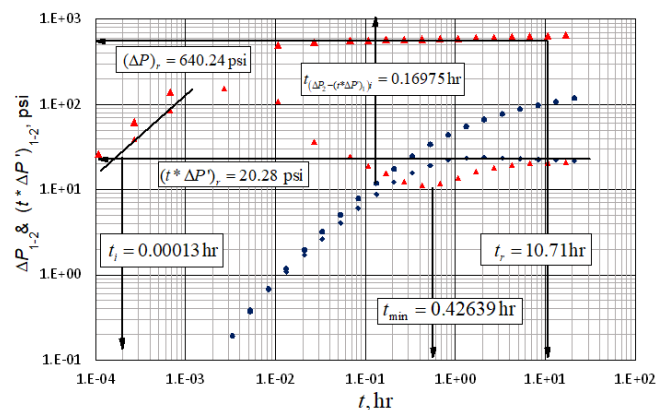


**Figure 9** Pressure and pressure derivative versus time log-log plot for the synthetic example.

**Table 3** Input data for synthetic example

$q = 200$ bpd	$r_w = 0.5$ ft	$B_o = 1.35$ rb/stb	$\phi_1 = 0.02$
$\phi_2 = 0.35$	$\mu = 0.7$	$c_t = 1 \times 10^{-5}$ psi-l	$h_1 = 100$ ft
$h_2 = 120$ ft	$\Delta h = 5$ ft		

The information below was read from Figure 9,

$$t_r = 202462 \text{ hr} \quad (t * \Delta P^*)_r = 0.2894 \text{ psi} \quad \Delta P_r = 10.48 \text{ psi}$$

$$t_i = 0.000028 \text{ hr} \quad t_{min} = 2.29 \text{ hr} \quad t_{(\Delta P_2 - (t * \Delta P^*)_1)} = 0.645 \text{ hr}$$

$$(t * \Delta P^*)_{min} = 0.1028 \text{ psi}$$

Estimate permeability with Equation (15);

$$k = \frac{70.6(200)(0.7)(1.35)}{(0.2894)(100)} = 461 \text{ md}$$

Find the value of  $\kappa$  with Equation (24) and  $k_1$  with Equation (25), respectively:

$$\kappa = 1.25 \times 10^{10} \left( \frac{(0.025)(0.7)(1 \times 10^{-5})(0.5^2)}{(461)(2.29)} \right) = 0.518$$

$$k_1 = 0.518 \left( \frac{(70.6)(200)(0.7)(1.35)}{(0.2894)(100)} \right) = 239 \text{ md}$$

Using the obtained value of  $k_1, k_2$  was calculated with Equation (18), yielding:

$$k_2 = \left( \frac{(70.6)(200)(0.7)(1.35)}{(0.2894)} - (239)(100) \right) \frac{1}{120} = 185 \text{ md}$$

Estimate  $\lambda$  and  $\omega$  using Equations (20) and (22), respectively:

$$\lambda = 2381.494 \left( \frac{(0.025)(0.7)(1 \times 10^{-5})(0.5^2)}{(239)(0.64)} \right) = 6.8 \times 10^{-7}$$

$$\omega = 6.584 \times 10^{-10} \left( \frac{(239)(0.64)}{(0.025)(0.7)(1 \times 10^{-5})(0.5^2)} \right)^{0.85} = 0.085$$

With the obtained  $\lambda$  value, find with Equation (9):

$$k_v = \frac{(6.8 \times 10^{-7})(5)[(239)(100) + (185)(120)]}{0.5^2} = 0.626 \text{ md}$$

Estimate wellbore storage and skin factor with Equations (16) and (17), respectively:

$$C = \frac{(239)(100)(0.000028)}{1695(0.7)} = 0.000564 \text{ bbl/psi}$$

$$s = 0.5 \left( \frac{10.48}{0.2894} - \ln \left[ \frac{(239)(204362)}{(0.025)(0.7)(1 \times 10^{-5})(0.5^2)} \right] + 7.43 \right) = 4.5$$

Results for this example are reported in Table 4 and are compared against input data.

**Table 4** Comparison of results for synthetic example

Parameter	Results from:	
	Input value	This work
$\kappa$	0.5314	0.518
$\omega$	0.0562	0.085
$\lambda$	$9.21 \times 10^{-7}$	$6.80 \times 10^{-7}$
$s$	0	4.5
$C$ , bbl/psi	0.0005	0.000564
$k_1$ , md	245	238
$k_2$ , md	180	185
$k_v$ , md	0.85	0.626

## Comments of the results

The results obtained in this study were analyzed by comparing the permeabilities of Zone 1 and Zone 2 estimated using the proposed TDS-based methodology with those reported by Ehlig-Economides & Ayoub,<sup>13</sup> who determined these parameters using a traditional interpretation procedure based on type-curve matching. In both cases, Tables 2 and 4 corresponding to the field and synthetic examples allow for a direct comparison of the estimated values and provide a basis to assess the impact of the interpretation methodology on the resulting reservoir parameters.

In the reference example presented by Ehlig-Economides & Ayoub,<sup>13</sup> the permeability of each zone was obtained through an iterative graphical matching process between the dimensionless pressure responses and previously generated families of type curves. Although this procedure is fully consistent with the underlying physical model, it relies on the visual selection of the curve that best fits the data, which inherently introduces a degree of subjectivity into the parameter estimation process. Under this approach, the permeability of Zone 1 is inferred from the early-time response dominated by the active layer, whereas the permeability of Zone 2 is estimated from the late-time behavior associated with vertical interference and crossflow between layers.

The results obtained for the field example also provide useful insight into the hydraulic interaction between the two layers. The estimated permeabilities indicate that Zone 1 exhibits a higher horizontal transmissibility than Zone 2, which explains why the early-time response of the pressure derivative is primarily controlled by the producing layer. As the transient evolves, the pressure disturbance propagates through the low-permeability barrier and induces crossflow between the layers. This interaction is reflected in the deviation of the derivative curve from the early radial-flow behavior and in the characteristic features used for parameter estimation. The relatively small value of the vertical communication parameter obtained in this case indicates that the separating layer offers significant resistance to vertical flow, which is consistent with the delayed interaction between the zones observed in the pressure-derivative response. These results confirm that the methodology captures the main hydraulic mechanisms governing vertical interference in stratified reservoirs.

The synthetic example further confirms the validity of the proposed methodology because the reservoir parameters imposed in the numerical model are known a priori. Under these controlled conditions, the interpretation procedure successfully reproduces the main properties of the system, including the permeabilities of the two layers and the vertical communication parameter. The close

agreement between the estimated parameters and the imposed input values demonstrates that the characteristic points identified on the pressure-derivative curves are consistent with the underlying physical model. This result indicates that the normalization procedures and analytical relationships developed in this study correctly capture the scaling behavior of the vertical interference system and can therefore be used with confidence for parameter estimation when the pressure transient response follows the theoretical model.

When the *TDS* technique developed in this work is applied to the same dataset, the estimated permeabilities for both zones are found to be of the same order of magnitude as those reported by Ehlig-Economides & Ayoub,<sup>13</sup> confirming the internal consistency of the adopted mathematical model. However, unlike the type-curve approach, the *TDS* methodology enables permeability estimation through the direct calculation of the parameter  $\kappa$  using clearly identifiable characteristic points on the pressure-derivative curve, without the need for graphical curve matching or subjective curve selection.

The numerical differences observed between the permeabilities obtained using the *TDS* technique and those reported by Ehlig-Economides & Ayoub,<sup>13</sup> are primarily associated with the interpretation approach employed in each case. In particular, the type-curve method used by the original authors yielded a permeability for Zone 2 that is closer to the reference value in the analyzed example, highlighting the effectiveness of graphical matching when sufficient data are available and the interpretation is carried out by an experienced analyst. Nevertheless, this procedure admits multiple acceptable solutions depending on the analyst's judgment. In contrast, the *TDS* technique leads to a unique solution based on the objective identification of characteristic points in the transient pressure response, thereby reducing interpretational ambiguity and improving result reproducibility, even though this does not necessarily guarantee a closer numerical match in all cases.

For the synthetic example, the application of the *TDS* technique successfully reproduced the permeabilities imposed in the numerical model, confirming its ability to estimate physically meaningful system parameters under controlled conditions. This outcome reinforces the advantage of the proposed methodology over traditional approaches, as the interpretation is performed in a direct and analytical manner without reliance on visual curve matching, even though the underlying physical model remains unchanged.

From a physical perspective, the estimated parameters provide a quantitative description of the hydraulic interaction between the layers. The permeability values of Zones 1 and 2 determine the relative horizontal flow capacities of each layer and therefore control how the pressure disturbance propagates radially from the well. The parameter  $\kappa$  reflects the contrast between these flow capacities and governs the redistribution of flow between the zones during the transient period. The storage parameter  $\omega$  describes the relative ability of each layer to store and release fluid through compressibility effects, influencing the duration of the early transient regime. Finally, the vertical communication parameter  $\lambda$  characterizes the transmissibility of the low-permeability barrier separating the layers and therefore controls the magnitude and timing of crossflow between the zones. Together, these parameters provide a comprehensive description of the dynamic behavior of the stratified system and allow the pressure-transient response to be interpreted in terms of the underlying reservoir properties.

Overall, the analysis demonstrates that while the mathematical model adequately describes the vertical interference phenomenon,

the *TDS*-based methodology represents a substantial improvement in the interpretation process. By enabling the direct estimation of zone permeabilities and reducing the subjectivity inherent in type-curve methods, the *TDS* technique provides a more robust and reproducible tool for the hydraulic characterization of stratified reservoirs with crossflow.

## Conclusions

1. An analytical methodology based on Tiab's Direct Synthesis (*TDS*) technique was developed for the interpretation of vertical interference tests in stratified systems with permeability contrasts. The proposed approach enables an objective characterization of hydraulic communication between layers during the pressure transient regime by translating the measured response into analytical relationships with sound physical and mathematical foundations.

The analysis of the vertical interference model demonstrated that the transient pressure response is governed by dimensionless parameters that represent the hydraulic contrast between zones rather than independent physical properties. In this context, the parameters  $\kappa$ ,  $\omega$ , and  $\lambda$  condense the interaction between layers with different flow and storage capacities, allowing the coupled behavior of the system to be described in a compact and consistent manner.

During the radial flow regime, the pressure derivative converges to a unique response controlled by the total flow capacity of the system. Consequently, the permeability estimated in this regime corresponds to an equivalent value that integrates the contribution of both zones, rather than the individual permeability of the producing layer. Using this equivalent permeability together with the parameter  $\kappa$ , the proposed methodology enables the analytical recovery of the individual permeabilities of each zone.

The parameter  $\kappa$  was identified as a central element of the methodology, since its direct determination from the pressure-derivative function allows the coupled system response to be decoupled without resorting to graphical matching procedures. In addition, it was shown that the use of the dimensionless time  $t_D$  is more appropriate than the vertical dimensionless time  $t_{vD}$  within the *TDS* framework, as it avoids double weighting of the composite system and preserves consistency with both the original model formulation and the pressure response measured in the active zone.

The application of the proposed methodology to both field and synthetic examples demonstrated that the main reservoir parameters can be reliably estimated from the characteristic points of the pressure-derivative response. In the field example, the permeabilities of the two layers obtained with the *TDS*-based methodology were consistent with those reported by Ehlig-Economides & Ayoub,<sup>13</sup> showing comparable magnitudes for the horizontal permeabilities and the vertical communication parameter. Considering the intrinsic sensitivity of parameters such as  $\kappa$ ,  $\omega$ , and  $\lambda$  in stratified and naturally fractured systems, the results obtained fall within the expected order of magnitude of the reference solution. In the synthetic example, the methodology reproduced the imposed model parameters with the same order of magnitude, confirming that the proposed analytical relationships provide physically consistent estimates of permeability contrast, storage capacity ratio, and vertical communication between layers.

## Acknowledgements

The authors acknowledge the use of the artificial intelligence tool **Gemini (Google)** for assisting in the generation of the conceptual illustration included in Figure 1. This tool was employed exclusively

for graphical purposes. All scientific content, modeling, analysis, and interpretation presented in this study were developed and validated by the authors.

## Conflicts of interest

The authors declare that there are no conflicts of interest.

## Nomenclature

$C_t$	Compressibility, psi-1
$B_o$	Oil volumen factor, rb/STB
$C$	Wellbore storage coefficient, bbl/psi
$c_t$	Total system compressibility, psi-1
$k$	Horizontal permeability, md
$K_0$	Modified Bessel function of v order
$K_1$	Modified Bessel function of v order
$h$	Reservoir thickness, ft
$P$	Pressure, psi
$q$	Flow rate, bpd
$r_w$	Wellbore radius, ft
$\mathcal{S}$	Laplace variable
$\mathcal{S}$	Skin
$t$	Time, hr
$(t * \Delta P')$	Presure derivative function, psi

## Greek

$K$	Permeability ratio
$\omega$	Porosity–compressibility–thickness coefficient
$\lambda$	Vertical communication factors
$\mu$	Viscosity, cp

## Suffixes

min	Mínimum
$t_{(\Delta P'_{i-1} - (t * \Delta P')_i)}$	Intercepto of $\Delta P'$ in zone 2 with in zone 1
$D$	Dimensionless
$r$	Radial
$v$	Vertical

## References

- Earlougher RC. Analysis and design methods for vertical well testing. *Journal of Petroleum Technology*. 1980;32(3):505–514.
- Tiab D, Kumar A. Application of the p'D function to interference analysis. *Journal of Petroleum Technology*. 1980;32(8):1465–1470.
- Theis C. The relation between the lowering of the piezometric surface and the rate and duration of discharge of a well using ground–water storage. *Eos, Transactions American Geophysical Union*. 1935;16(2):519–524.
- Muskat M. *The Flow of Homogeneous Fluids Through Porous Media*. Edwards Brothers Inc; 1946.
- Van Everdingen AF, Hurst W. The application of the Laplace transformation to flow problems in reservoirs. *Journal of Petroleum Technology*. 1949;1(12):305–324.
- Horner DR. Pressure build–up in wells. In: *Proceedings of the Third World Petroleum Congress*. 1951:503–523.
- Cooper HH Jr, Jacob CE. A generalized graphical method for evaluating formation constants and summarizing well–field history. *Eos, Transactions American Geophysical Union*. 1946;27(4):526–534.
- Gringarten AC, Ramey HJ Jr. The use of source and Green's functions in solving unsteady–flow problems in reservoirs. *Society of Petroleum Engineers Journal*. 1973;13(5):285–296.
- Burns WA. New single–well test for determining vertical permeability. *Journal of Petroleum Technology*. 1969;21(6):743–752.
- Prats M. A method for determining the net vertical permeability near a well from in–situ measurements. *Journal of Petroleum Technology*. 1970;22(5):637–643.
- Hirasaki GJ. Pulse tests and other early transient pressure analyses for in–situ estimation of vertical permeability. *Society of Petroleum Engineers Journal*. 1974;14(1):75–90.
- Bremer RE, Winston H, Vela S. Analytical model for vertical interference tests across low–permeability zones. *Society of Petroleum Engineers Journal*. 1985;25(3):407–418.
- Ehlig–Economides C, Ayoub JA. Vertical interference testing across a low–permeability zone. *SPE Formation Evaluation*. 1986;1(5):497–700.
- Hatzignatiou DG, Ogbe DO. Interference pressure behavior in stratified reservoirs. In: *SPE Western Regional Meeting*. Society of Petroleum Engineers; 1993.
- Bourdet D. Well test analysis: *The use of advanced interpretation models*. Elsevier; 2002.
- Kuchuk FJ. *Transient Pressure Analysis for Well Testing*. Society of Petroleum Engineers; 2014.
- Tiab D, Donaldson EC. *Petrophysics: Theory and Practice of Measuring Reservoir Rock and Fluid Transport Properties*. 4th ed. Gulf Professional Publishing; 2015.
- Tiab D. Analysis of pressure and pressure derivative without type–curve matching—III: vertically fractured wells in closed systems. In: *SPE Western Regional Meeting*. Society of Petroleum Engineers. 1993.
- Tiab D. Analysis of pressure and pressure derivative without type–curve matching—skin and wellbore storage. *Journal of Petroleum Science and Engineering*. 1995;12(3):171–181.
- Escobar FH, Sánchez Murcia W, Montealegre M. Characterization of a stratified reservoir with cross flow using Tiab's direct synthesis (TDS) technique. *Journal of Mineral and Material Science (JMMS)*. 2025;6(3):1–6.
- Mendoza IA. *Interpretación de Pruebas de Interferencia Vertical Para Zonas de Diferente Permeabilidad*. 2026.
- Escobar FH, Bonilla LF, Hernández CM. A practical calculation of the distance to a discontinuity in anisotropic systems from well test interpretation. *DYNA*. 2018;85(207):65–73.